

## Article

# A Stochastic Planning Model for Battery Energy Storage Systems Coupled with Utility-Scale Solar Photovoltaics

Heejung Park

School of Energy Engineering, Kyungpook National University, Daegu 41566, Korea; h.park@knu.ac.kr

**Abstract:** With recent technology advances and price drop, battery energy storage systems (BESSs) are considered as a promising storage technology in power systems. In this paper, a stochastic BESS planning model is introduced, which determines optimal capacity and durations of BESSs to co-locate utility-scale solar photovoltaic (PV) systems in a high-voltage power system under the uncertainties of renewable resources and electric load. The optimization model minimizing total costs aims to obtain at least 20% electric energy from renewable sources, while satisfying all the physical constraints. Furthermore, two-stage stochastic programming is applied to formulate mathematical optimization problem to find out optimal durations and capacity of BESSs. In scheduling BESSs, chronology needs to be considered to represent temporal changes of BESS states; therefore, a scenario generation method to generate random sample paths with 1-h time step is adopted to explicitly represent uncertainty and temporal changes. The proposed mathematical model is applied to a modified IEEE 300-bus system that comprises 300 electric buses and 411 transmission lines. Optimal BESS durations and capacity are compared when different numbers of scenarios are employed to see the sensitivity to the number of scenarios in the model, and “value of stochastic solution” (VSS) is calculated to verify the impacts of inclusion of stochastic parameters. The results show that the building costs and capacity of BESSs increase when the number of scenarios increases from 10 to 30. By inspecting VSSs, it is observed that an explicit representation of stochastic parameters affects the optimal value, and the impacts become larger when the larger number of scenarios are applied.

**Keywords:** power system planning; stochastic optimization; utility-scale energy storage; renewable energy; solar PV; power system simulation



**Citation:** Park, H. A Stochastic Planning Model for Battery Energy Storage Systems Coupled with Utility-Scale Solar Photovoltaics. *Energies* **2021**, *14*, 1244. <https://doi.org/10.3390/en14051244>

Academic Editor: Pavlos Georgilakis

Received: 14 January 2021  
Accepted: 15 February 2021  
Published: 24 February 2021

**Publisher's Note:** MDPI stays neutral with regard to jurisdictional claims in published maps and institutional affiliations.



**Copyright:** © 2021 by the author. Licensee MDPI, Basel, Switzerland. This article is an open access article distributed under the terms and conditions of the Creative Commons Attribution (CC BY) license (<https://creativecommons.org/licenses/by/4.0/>).

## 1. Introduction

Energy storage systems (ESSs) generally have been used as a means for shifting peak load by supplying electricity during peak load hours with stored energy. Therefore, the discrepancy between the peak and base loads decreases, and low load levels and electricity prices are ensured.

Recently, a considerable attention is devoted to the planning and operation of ESSs, especially for battery energy storage systems (BESSs) that store electric energy in the form of chemical energy for dealing with the uncertainty and intermittency of increased renewable resources in the power system, as well as shaving the peak load. As of 2018, global installed capacity of BESSs is approximately 170 GW and expected to increase further [1]. The rapidly evolving technology and declining costs of BESSs are the main drivers of the extensive utilization of BESSs. In this context, well-defined simulation tools for planning capacity of BESSs in a power system need to be developed to estimate costs and assess effectiveness of BESS installation. Therefore, mathematical optimization models are studied to obtain optimal capacity of BESSs to meet specific criteria of given power systems such as environmental energy policies.

In literature, the BESSs have been mainly used for load leveling in the early stage. In that context, optimal capacity of BESSs is evaluated with mathematical optimization model [2].

From the perspective of promoting generation from renewable sources, BESSs may provide us with applicable and effective solutions for mitigating the uncertainty associated with renewable energy sources. Therefore, BESS simulation models for power systems containing renewable energy sources are being continuously studied. The models in which BESSs are scheduled in a short-term period are developed to evaluate impacts of operating BESSs, with generators using renewable energy [3], where security-constrained unit commitment decision is included in the operating problem. Furthermore, a simulation model is introduced for evaluating optimal hybrid energy system, including solar PVs, wind turbines, battery banks, and fuel cells [4], which focuses on seeking an optimal level of renewable generation capacity and optimal capacity of battery systems.

Capacity planning for grid-connected PV systems using a multi-objective optimization approach for obtaining a solution to meet multiple criteria has been studied previously in [5]. A near optimal solution is found heuristically using a generic algorithm.

Another model to simulate optimal capacity of BESSs for a small-scale power system has been presented in [6], where representative hourly scenarios for wind power and deterministic load are implemented to determine the size of BESSs. The result was intended to be utilized for the subsequent network planning or generation capacity planning, so that a network model is not employed, and power flow is not verified. Talent and Du discussed a model for optimal capacity of solar PVs and battery in a previous study [7], where the reduction in the payment amounts of consumers with respect to their electricity bills are maximized. Furthermore, a case study is conducted with a residential-level electric grid, which is not fully described in the form of electric buses and distribution lines.

On designing PV systems with BESSs, a model to minimize the total costs for installations and operations is presented in [8]. Within the lifetime of BESSs, the effect of BESS installation is investigated when installing, operating, replacing and divesting the PV systems.

An optimization model is suggested to determine optimal size of the BESSs for a hybrid power system with wind, solar, and BESSs [9]. A small-scale power system that can be connected or disconnected to the grid depending on the operation mode is applied for the simulation.

A stochastic model to optimize the storage systems installed together with PV generation systems is described in [10]. The optimal capacity of BESSs coupled with residential-scale PV systems is assessed using a stochastic model for home energy management systems. Therefore, power grid is not included in the model.

From a different view of mathematical programming, robust optimization can be implemented for mathematical formulation. Several models for optimal capacity of ESSs in transmission and distribution systems are found in [11,12]. In selecting a method for mathematical programming, robust optimization can be an alternative offering a tractable optimization problem without known probability distributions of uncertain factors. Therefore, real-world problems that the probability distributions are generally unknown can be modelled with robust optimization. However, an obtained solution can be “robust” because typical robust optimization problems are solved with respect to uncertainty sets that comprise worst-case realizations. On the other hand, stochastic programming is based on the known probability distributions, and probabilistic characteristics of uncertain parameters are explicitly represented. In this paper, a method to consider probability distribution and autocorrelation is applied for probability modeling of uncertain factors.

The recent growth in utility-scale PV capacity is significant. The U.S. Energy Information Administration (EIA) expected new capacity addition of 13 GW in 2020 and 11 GW in 2021, respectively [13]. However, solar PV generation does not always increase proportionally in accordance with PV capacity additions, because the availability of solar power is strictly limited to daytime. Furthermore, the PV generation needs to be curtailed in some circumstances. With a large amount of PV generation capacity, one solution to utilize the available PV capacity can be installing BESSs coupled with solar PVs, and that configuration can be said to be “dispatchable”. In this context, it is important to figure

out how much capacity of BESSs can effectively improve the utilization of solar PVs and provide more dispatchable characteristics.

Despite the needs in the investigation of BESS capacity, optimal level of utility-scale BESSs with PV systems in a power system is not well studied. The optimization models in literature merely focus on PV systems in a small-scale grid at a residential level, and BESSs with utility-scale PVs operated in a large-scale grid are not included in those models. Therefore, in this study, optimal duration and capacity of BESSs coupled with utility-scale solar PVs required to maintain a certain level of renewable energy generation versus electric load are examined with a stochastic optimization model.

The general perception of renewable resources from a modeling perspective can be characterized by intermittency and uncertainty. Any simulation model including renewable resources needs to represent the stochasticity of them, and modeling techniques for uncertainty of renewable resources also need to be applied subsequently. Furthermore, scheduling problems consider chronology, and the level of temporal information described is high. Therefore, the optimization models involving scheduling require high computational efforts and are sometimes intractable when the level of details is excessively high. The optimization model presented in this paper comprises the aspects of stochastic models for planning and operation.

The contributions of this paper can be summarized as follows.

- A stochastic utility-scale BESS capacity planning model for solar PV systems considering uncertainty and chronology is introduced.
- Uncertain factors, solar DNI, wind power availability, electric load, are modeled as stochastic processes capturing uncertainty and time order of the factors, and the random sample paths for scenarios in the stochastic optimization problem are generated using the stochastic process.
- The presented model is applied to a transmission-level 300-bus power system, and an optimal solution is obtained.
- The impact of inclusion uncertainty in the BESS capacity planning model is investigated using the idea, “Value of Stochastic Solution” (VSS) [14].

The rest of the paper is organized as follows. In Section 2, a method to generate sample paths and a mathematical formulation to optimize capacity of BESSs are introduced. The costs, a power system model applied to the mathematical model, and the assumptions for simulation are described in the subsequent section. Optimal BESSs capacity obtained from the presented model and some results analysis are presented in Section 4. Finally, discussions and conclusions are stated in Sections 5 and 6.

## 2. Methodology

### 2.1. Sample Path Generation

The main factors exhibiting natural uncertainty are considered as uncertain parameters in the simulation model; they are wind power availability, solar irradiance, and electric load in this study. As an optimization problem involving chronological scheduling is formulated, a method to generate sample paths needs to be implemented which represents uncertainty and chronology simultaneously. For that purpose, autoregressive-to-anything (ARTA) process is applied [15,16] to generate hourly random sample paths using autocorrelations and marginal distributions of uncertain parameters. Generally, the empirical data of random parameters are not stationary, so that the procedure for finding an ARTA process is modified to generate stationary data from the original data set. The procedure is briefly described below, and the whole procedure with more details can be found in a previous study [17].

The procedure can be summarized as forming a base stationary process  $\{Z_t\}$  with autocorrelations and marginal distributions derived from the corresponding historical time-series data, generating sample paths  $Z_t^\omega$  with initial values  $Z_{t-1}^\omega, Z_{t-2}^\omega, \dots, Z_{t-p}^\omega$ , and transforming  $Z_t^\omega$  into the desired sample path  $\zeta_t^\omega$ . The procedure of generating  $N$  sample paths is provided in this section. AR(2) base process with lag 2 is used, and sample paths for 24 h with a 1-h interval are generated through the following steps.

1. The desired process  $\{\xi_t\}$  is not stationary in general; therefore, the intermediate process  $\{\bar{\xi}_t\}$  satisfying  $\bar{\xi}_t = \xi_{t+1} - \xi_t, t = 1, 2, \dots, T - 1$  is defined here, which is stationary. The autocorrelation structure and marginal distribution of the intermediate process,  $\rho = (\rho_1, \rho_2, \dots, \rho_p)$  and  $F$ , are known, where  $\rho_p = \text{Corr}[\bar{\xi}_t, \bar{\xi}_{t+p}]$ , and  $p$  indicates lag.
2. With the autocorrelation structure in Step (1), the AR parameters  $\alpha_p$  and the variance  $\sigma^2$  are obtained. The ARTA process with  $p = 2$  is implemented throughout the simulation, therefore,  $\rho = (\rho_1, \rho_2)$  and  $\alpha_1, \alpha_2$  are obtained.
3. A base AR(2) process  $Z_t = \alpha_1 Z_{t-1} + \alpha_2 Z_{t-2} + \epsilon_t$  is formed, where  $Z_t \sim N(0, 1)$  and  $\epsilon_t \sim N(0, \sigma^2)$ .
4. Generate  $Z_t^{\omega_1}, t = 0, 1, \dots, 23$  for 24 h using the initial values  $Z_{-1}^{\omega_1}, Z_{-2}^{\omega_1}$ .
5. The intermediate value  $\bar{\xi}_t^{\omega_1}$  can be derived with  $\bar{\xi}_t^{\omega_1} = F^{-1}[\Phi(Z_t^{\omega_1})]$ . Finally, the desired process  $\xi_t^{\omega_1}$  is obtained from  $\xi_t^{\omega_1} = \bar{\xi}_t^{\omega_1} + \xi_{t-1}^{\omega_1}$ .
6. Repeat Steps (1)–(5) for  $\omega_2, \omega_3, \dots, \omega_N$ .

## 2.2. Mathematical Model

In this section, a mathematical formulation of the stochastic BESS capacity planning problem is presented, where the formulation is done with two-stage stochastic programming [14,18]. Instead of a primitive form of the formulation with stochastic programming, an approximated, deterministic equivalent problem is provided for a clear presentation of the cost terms.

$$\begin{aligned} \min \alpha_b x_b + \sum_{\omega \in \Omega} p^\omega \left[ \sum_{t \in \mathbf{T}} h_t \left( \sum_{g \in \mathbf{G}} o_g P_{tg}^\omega + \sum_{c \in \mathbf{G}^c} o_c^r R_{tc}^\omega \right. \right. \\ \left. \left. + \sum_{b \in \mathbf{B}} (o_b C Q_{tb}^\omega + o_b D Q_{tb}^\omega) \right. \right. \\ \left. \left. + \beta \sum_{d \in \mathbf{D}} U D_{td}^\omega + \beta^r U R_t^\omega \right) + \gamma \cdot U R P S^\omega \right] \end{aligned} \quad (1)$$

subject to

$$0 \leq x_b \leq P_b^{\max}, \quad \forall b \in \mathbf{B} \quad (2)$$

$$\sum_{b \in \mathbf{B}} \Lambda_{sb} \cdot x_b \leq P_s^{\max}, \quad \forall s \in \mathbf{S} \quad (3)$$

$$P_{tc}^\omega + R_{tc}^\omega \leq P_c^{\max}, \quad \forall \omega \in \Omega, \forall t \in \mathbf{T}, \forall c \in \mathbf{G}^c \quad (4)$$

$$P_{ts}^\omega + \sum_{b \in \mathbf{B}} \Lambda_{sb} \cdot C Q_{tb}^\omega \leq P_s^{\max}(\xi^\omega), \\ \forall \omega \in \Omega, \forall t \in \mathbf{T}, \forall s \in \mathbf{G}^s \quad (5)$$

$$P_{tw}^\omega \leq P_w^{\max}(\xi_{wt}^\omega), \quad \forall \omega \in \Omega, \forall t \in \mathbf{T}, \forall w \in \mathbf{G}^w \quad (6)$$

$$\sum_{g \in \mathbf{G}} \Lambda_{gi} \cdot P_{tg}^\omega - \sum_{l \in \mathbf{L}} \Lambda_{li} \cdot f_{tl}^\omega + \sum_{d \in \mathbf{D}} \Lambda_{di} \cdot U D_{td}^\omega \\ + \sum_{b \in \mathbf{B}} \Lambda_{bi} \cdot D Q_{tb}^\omega = \sum_{d \in \mathbf{D}} \Lambda_{di} \cdot P_d^{\max}(\xi_{dt}^\omega), \\ \forall \omega \in \Omega, \forall t \in \mathbf{T}, \forall i \in \mathbf{I} \quad (7)$$

$$Q_{tb}^\omega = Q_{t-1,b}^\omega + \eta_b \cdot C Q_{tb}^\omega - D Q_{tb}^\omega, \\ \forall \omega \in \Omega, \forall t \in \mathbf{T}, \forall b \in \mathbf{B} \quad (8)$$

$$0 \leq Q_{tb}^\omega \leq x_b \cdot e_b, \quad \forall \omega \in \Omega, \forall t \in \mathbf{T}, \forall b \in \mathbf{B} \quad (9)$$

$$0 \leq DQ_{tb}^\omega \leq x_b, \quad \forall \omega \in \Omega, \forall t \in \mathbf{T}, \forall b \in \mathbf{B} \quad (10)$$

$$0 \leq CQ_{tb}^\omega \leq x_b / \eta_b, \quad \forall \omega \in \Omega, \forall t \in \mathbf{T}, \forall b \in \mathbf{B} \quad (11)$$

$$\sum_{c \in \mathbf{G}^c} R_{tc}^\omega + UR_t^\omega \geq RS \sum_{g \in \mathbf{G}} P_{tg}^\omega, \quad \forall \omega \in \Omega, \forall t \in \mathbf{T} \quad (12)$$

$$\begin{aligned} & \sum_{t \in \mathbf{T}} \left( \sum_{s \in \mathbf{S}} P_{ts}^\omega + \sum_{w \in \mathbf{W}} P_{tw}^\omega + \sum_{b \in \mathbf{B}} DQ_{tb}^\omega \right) + URPS^\omega \\ & \geq RPS \cdot \sum_{t \in \mathbf{T}} \sum_{d \in \mathbf{D}} (P_d^{max}(\zeta_{dt}^\omega) - UD_{td}^\omega), \quad \forall \omega \in \Omega \end{aligned} \quad (13)$$

$$-f_l^{max} \leq f_{tl}^\omega \leq f_l^{max}, \quad \forall \omega \in \Omega, \forall t \in \mathbf{T}, \forall l \in \mathbf{L} \quad (14)$$

$$f_{tl}^\omega - \sum_{i \in \mathbf{I}} S_{li} \frac{\theta_{li}^\omega}{X_l} = 0, \quad \forall \omega \in \Omega, \forall t \in \mathbf{T}, \forall l \in \mathbf{L} \quad (15)$$

$$-\frac{\pi}{2} \leq \sum_{i \in \mathbf{I}} S_{li} \theta_{li}^\omega \leq \frac{\pi}{2}, \quad \forall \omega \in \Omega, \forall t \in \mathbf{T}, \forall l \in \mathbf{L} \quad (16)$$

$$0 \leq UD_{td}^\omega \leq P_d(\zeta_{dt}^\omega), \quad \forall \omega \in \Omega, \forall t \in \mathbf{T}, \forall d \in \mathbf{D} \quad (17)$$

$$-\pi \leq \theta_{ti}^\omega \leq \pi, \quad \forall \omega \in \Omega, \forall t \in \mathbf{T}, \forall i \in \mathbf{I} \quad (18)$$

$$P_{tg}^\omega, R_{tc}^\omega, UR_t^\omega, URPS^\omega, CQ_{tb}^\omega, DQ_{tb}^\omega, Q_{tb}^\omega \geq 0. \quad (19)$$

In a two-stage stochastic programming framework, the building decisions of BESSs are made under the uncertainty of wind and solar power availability and electric demand. Subsequently, hourly operating decisions, such as optimal power flow, and charging and discharging operations of BESSs, are made with respect to realization of the uncertainties.

In (1), the objective function is represented by the sum of cost terms for building BESSs, operating generators and BESSs, penalty costs for failure of serving electricity demand, procuring capacity reserve, and meeting RPS requirements. The applied numeric values for these penalty costs are \$30,000/kWh, \$1000/kWh, and \$300/kWh, respectively, and the reserve procurement costs are assumed as 1/10 of the operating costs of generators.

Constraints (2) restrict the maximum capacity of BESSs to a given value, which is set to 100 MW to match the individual capacity of a solar PV farm. Within 100 MW, the capacity of BESSs can be determined to minimize the total cost. The building decision variable  $x_b$  is modeled as a continuous variable so that the exact required capacity can be obtained. One solar PV farm has three candidate BESSs with different durations: 1 h, 2 h, and 4 h. The total capacity to be installed is 100 MW. Therefore, the sum of three types of BESS capacity is 100 MW in (3), where  $P_b^{max}$  is 100 MW, regardless of the types of BESSs,  $b$ , in this simulation. Conventional generators that can be dispatched according to the system requirements provide capacity reserve throughout the planning horizon, and the reserved capacity plus energy cannot exceed their fixed capacity in (4). Because the unit commitment decision is not included in the optimization model, reserves can be procured from a generator regardless of whether the generator is dispatched.

The sum of power injection from solar PVs, and storing power into BESSs must be less than or equal to the solar power availability of the solar farm which is described in (5), where the solar power availability is estimated with respect to a randomly generated DNI sample path ( $\zeta^\omega$ ) at the given time  $t$  (for calculation of the solar power availability, see [19,20]). The power injection from a wind farm  $w$  to the grid,  $P_{tw}^\omega$ , is limited subject to the wind power availability based on the constraints (6). When the wind power injection is less than the wind power availability, there exist wind power curtailments. At each bus, the sum of injected power generation from any types of generators, power flow through the transmission lines, and discharged power from the BESS is the same as the served electric demand, i.e., the electricity demand subtracted by unserved amounts (7).

The total stored energy in a BESS at time  $t$  is represented by the sum of energy stored at time  $t - 1$ , and the charging and discharging amounts of energy at time  $t$ , where the round-trip efficiency is multiplied by the amount of charging power in (8), indicating the

occurrence of losses during the charging operation. To avoid interseasonal storage and to assign a valid value to  $Q$  when  $t$  becomes 0,  $Q_{tb}^{\omega}$  is set to 0 for  $t = 0, 24, 48, 72, 96$ .

The stored energy is constrained by the built capacity times the BESS time duration  $x_b \times e_b$  depending on the selected BESS (9). The charging and discharging power at a given time  $t$  are limited in accordance with built capacity of the BESS in MW, and charging and discharging operation cannot occur simultaneously, due to the operating cost that is evenly incurred for each action. The corresponding constraints are described in (10) and (11). The efficiency,  $\eta_b$ , is assumed to be 0.85.

Based on constraints (12), a fixed rate of capacity reserve can be procured with respect to the amount of power injection and the reserve margin. In this simulation,  $RS$  is assumed to be 15% [21]. The reserve is not a short-term operating reserve, but rather a capacity margin that is considered from a system planning stage. It is assumed that only the thermal generators offer reserve capacity.

In (13), the power injections from the wind and solar PV farms and the discharged power from BESSs are greater than or equal to the RPS requirements on the right hand side, where the  $RS$  is set to 20%. The slack variable,  $URPS^{\omega}$ , is included to avoid the infeasibility of the constraints.

In (14), the power flow on line  $l$  is constrained by the physical capacity limit for the positive or negative direction of flows. The negative capacity value indicates that the flow is in the opposite direction with respect to the reference flow direction. The DC power flow is implemented to perform the calculations of real power flow in (15). The voltage angle difference between the buses linked with a transmission line is maintained less than  $90^{\circ}$  due to (16), where the given constraints are generally not violated. The unserved demand must be equal to or less than realized electricity demand at each time  $t$ .

The unserved demand cannot exceed the realized load; therefore, the constraints are added in the formulation in (17). Equation (18) restricts the upper and lower limits of the variable,  $\theta_{ii}^{\omega}$ , and all the decision variables appearing in (19) have non-negative values.

### 3. Simulation

In this section, the conditions for BESS capacity planning, such as costs and network model, and generators information are provided, including detailed assumptions. A widely implemented BESS technology, lithium-ion BESS is selected for the BESS model. Therefore, the characteristics of the BESS such as costs and efficiency are based on the lithium-ion BESS.

#### 3.1. Building and Operating Costs

Throughout the simulation, all the costs are evaluated with respect to 2018\$ value. The installation cost of a BESS for the target year 2030 is estimated according to previous studies [22,23] with the “high” case. The installation cost is observed to reduce by approximately 21% in 2030 when compared with that in 2018 for “high” case. Furthermore, the installation cost for a stand-alone BESS is applied to estimate the cost in a conservative way. Based on the projected installation costs, the annualized building costs for BESSs are calculated, where the lifetime of the BESS and a discount rate are assumed to be 15 years and 5%, respectively. The equivalent annual costs (EACs) associated with installation of BESSs are calculated as follows:

$$EAC = PR \times BC \times \frac{r}{1 - \frac{1}{(1+r)^n}}, \quad (20)$$

where  $PR$  and  $BC$  indicate the projection rate and over-night building cost, respectively. The parameters,  $r$  and  $n$ , represent the discount rate and lifetime of BESSs. The projection rate considered in this simulation is 0.79 [1], and the operating costs of BESSs are assumed to be \$0.3/MWh for charging and discharging operations, respectively.

The generation costs comprise variable operations and maintenance (VOM) costs and fuel costs. The heat rates obtained from different generation technologies, fuel costs in 2030,

and VOM costs are applied in accordance with the report [24]. The calculated costs for BESS installation and electric energy generation are presented in Table 1. Different types of BESSs indicate their charging and discharging durations. The BESS (2-h) can store electric energy up to its rated capacity times 2 h.

**Table 1.** Installation and operating costs of generators and battery energy storage systems (BESSs).

Technology Type	Equivalent Annual Installation Cost (\$/kW.year)	Operating Cost (\$/MWh)
Coal	-	28.93
Conv. CT	-	45.05
Adv. CT	-	52.30
CCGT	-	39.03
Nuclear	-	9.47
BESS (1-h)	45.74	0.3
BESS (2-h)	69.11	0.3
BESS (4-h)	115.69	0.3

### 3.2. Power System Model

The mathematical optimization model described in Section 2.2 was applied to a modified IEEE 300-bus system [25,26] to verify whether the model performs as planned. The installed capacity of the generating units based on their technology types, and the specified information of BESSs to be built is also listed in Table 2, where the types of generators are conventional combustion turbine (Conv. CT), advanced combustion turbine (Adv. CT), and combined cycle gas turbine (CCGT). The power system used in the simulation has 114 generators, including wind and solar PV farms. The unit capacity of solar PV farm is rated at 100 MW. The CCGT constitutes the highest proportion in terms of the installed capacity, and the capacity of wind and solar PVs reaches 7400 MW, which is about 27.6% of the total generating capacity. With the given capacity, it is assumed that 20% of the total electric energy is generated from renewable resources. For a reference case, electric demand is set to 14,651.42 MW. In the model, 411 high voltage transmission lines exist.

**Table 2.** Capacity of generating units.

Types of Generation	# of Units	Capacity (MW)	Percents (%)
Coal	6	3900	14.55
Conv. CT	8	2400	8.96
Adv. CT	10	2100	7.84
CCGT	15	9000	33.58
Nuclear	1	2000	7.46
Wind	35	3500	13.06
Solar	39	3900	14.55
Total	114	26,800	100

### 3.3. Hourly Random Sample Paths

Figure 1 presents historical data for the given uncertain parameters, where the top and bottom values on the vertical bar indicate the maximum and minimum values, respectively. The data for solar DNI are obtained from the website [27]. Wind power availability and electric load data are from the study [17]. The plots in blue and red indicate the median and mean values of each data, respectively. Hourly scenarios representing one year are generated from four different ARTA processes representing spring, summer, fall, and winter, where a sample path for a year contains 96 intervals. Figure 2 illustrates 20 sample paths together. For a comparison of impacts on optimal solutions due to a change of sample path number, 10, 20, and 30 paths are generated. The generated sample paths for electric load are scaled down to fit the 300-bus system by multiplying a fixed value, 0.35.

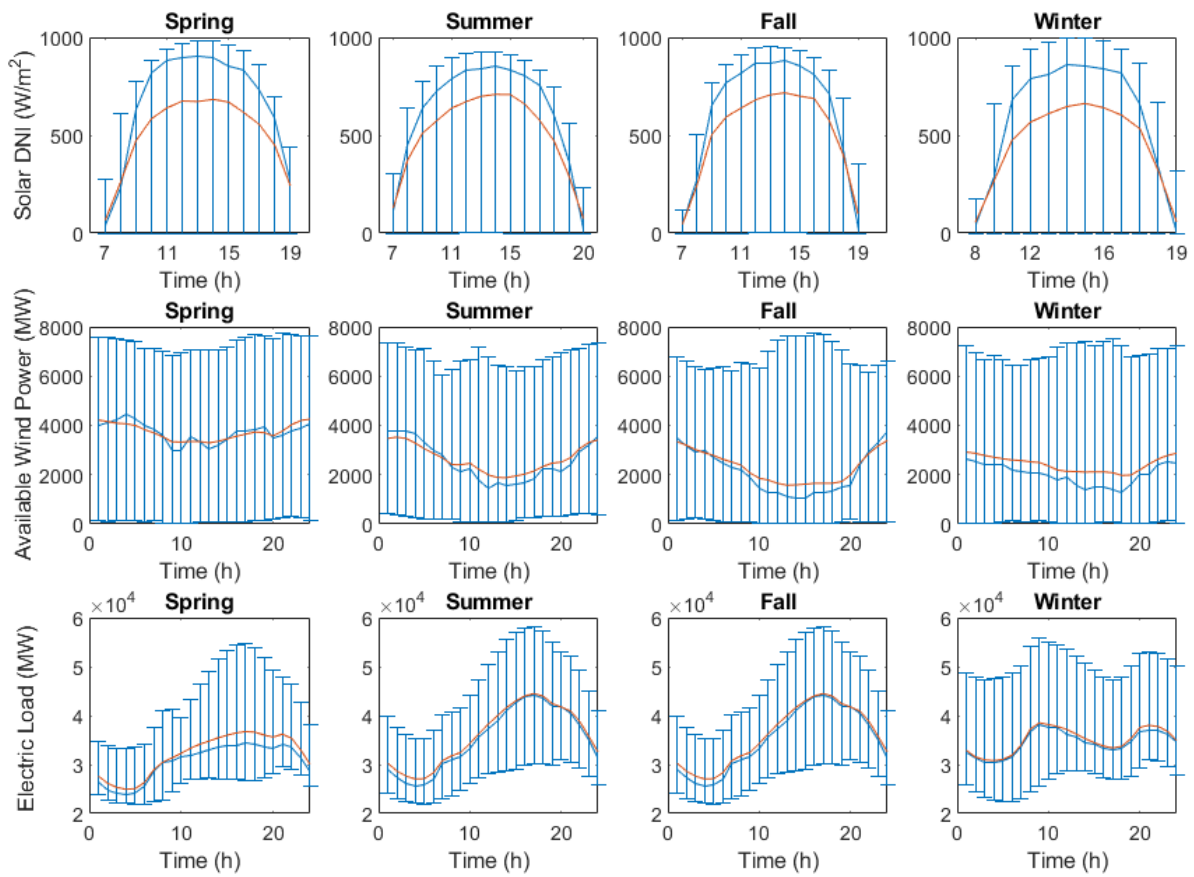


Figure 1. Historical data for solar DNI, wind power availability, and electric load [17,27].

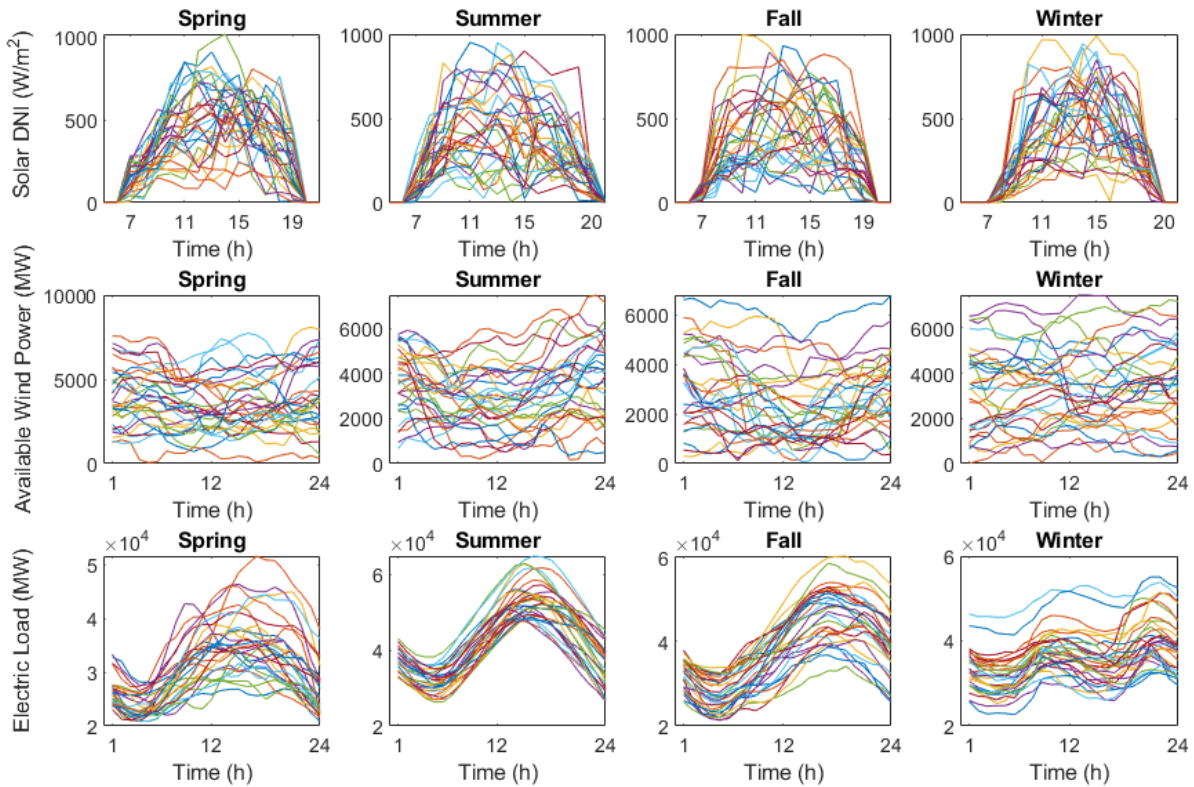


Figure 2. Generated hourly sample paths for four seasons with autoregressive-to-anything (ARTA) process.

#### 4. Simulation Results

Optimal solutions with the presented optimization model are found using GAMS/CPLEX [28]. A computing machine with two Intel 8-core 3.6 GHz Xeon Gold processors and 256 GB memory is used for calculation. The average computing times for obtaining optimal solutions with 10, 20, and 30 samples are 13,934.72, 290,901.16, and 315,852.84 s, respectively.

##### 4.1. Optimal Capacity and Costs for BESSs

Three types of BESSs with 1-, 2-, and 4-h durations are applied to the simulation to find optimal points of BESS capacity and durations at different locations. At each electrical bus, an individual solar PV has three candidate BESSs with different durations, and optimal capacity of the BESSs can be found with any combination of three candidate BESSs within 100 MW. The optimal BESS capacity in accordance with the duration is listed in Table 3, where the optimal solutions with 10, 20, and 30 sample paths are compared in order to see sensitivity associated with the number of sample paths. A larger capacity of BESSs can be built when 30 sample paths are applied compared to 10 and 20 sample paths. The BESSs with a long duration tend to be preferred for building as the number of sample paths increases.

In Table 4, the optimal costs are reported when different numbers of sample paths are applied. When the number of samples is increased, the optimization model selects to build more capacity of BESSs; therefore, the building cost increases. The presence of more sample paths results in higher variability in the model, and the amount of electric energy that certainly obtained from solar PVs decreases. Therefore, in the decision-making to build BESSs, it tends to build more capacity to cope with high variability and utilize more renewable energy when the number of sample paths increases. From the perspective of building solar PV generation systems, less capacity of solar PVs can be built when the short-term variability is considered or the number of sample paths increases [17].

**Table 3.** Optimal building capacity for BESSs with different numbers of samples (MW).

Duration	Number of Samples		
	10	20	30
1-h	3.25	4.24	53.97
2-h	885.86	19.49	202.88
3-h	3.82	1337.21	1466.55
Total	892.94	1360.94	1723.4

**Table 4.** Optimal building costs for BESSs with different numbers of samples (\$ million/year).

Duration	Number of Samples		
	10	20	30
1-h	0.0116	0.0152	0.1930
2-h	4.7856	0.1053	1.0960
3-h	0.0346	12.0928	13.2626
Total	4.8318	12.2133	14.5515

##### 4.2. Charging and Discharging Operations of BESSs

The average charging and discharging operations of the built BESSs and stored energy status are presented in Figure 3. The charged and discharged amounts are represented in electric energy for time  $t$ . The BESSs with optimal capacity obtained in Section 4.1 are built in the system, and an operating simulation is conducted with 30 additionally generated random sample paths. The resulting 30 operating plans at time  $t$  for each BESS are averaged, and the total amounts of charged and discharged energy for all BESSs are illustrated for time  $t$ . The initial states of BESSs are assumed to be 0 MWh for each season,

implying that the BESSs are not allowed to act as an inter-season energy storage. For any BESS, the charging and discharging operations do not occur simultaneously by adding a small amount of operating cost for both charging and discharging operations as stated in Section 2.2. During spring, summer, and fall, the charging operation occurs mainly before noon, which is the time in which solar PVs actively generates electricity. The load profile for winter indicates a different pattern compared with the other seasons, and the charging operation continues until 19:00.

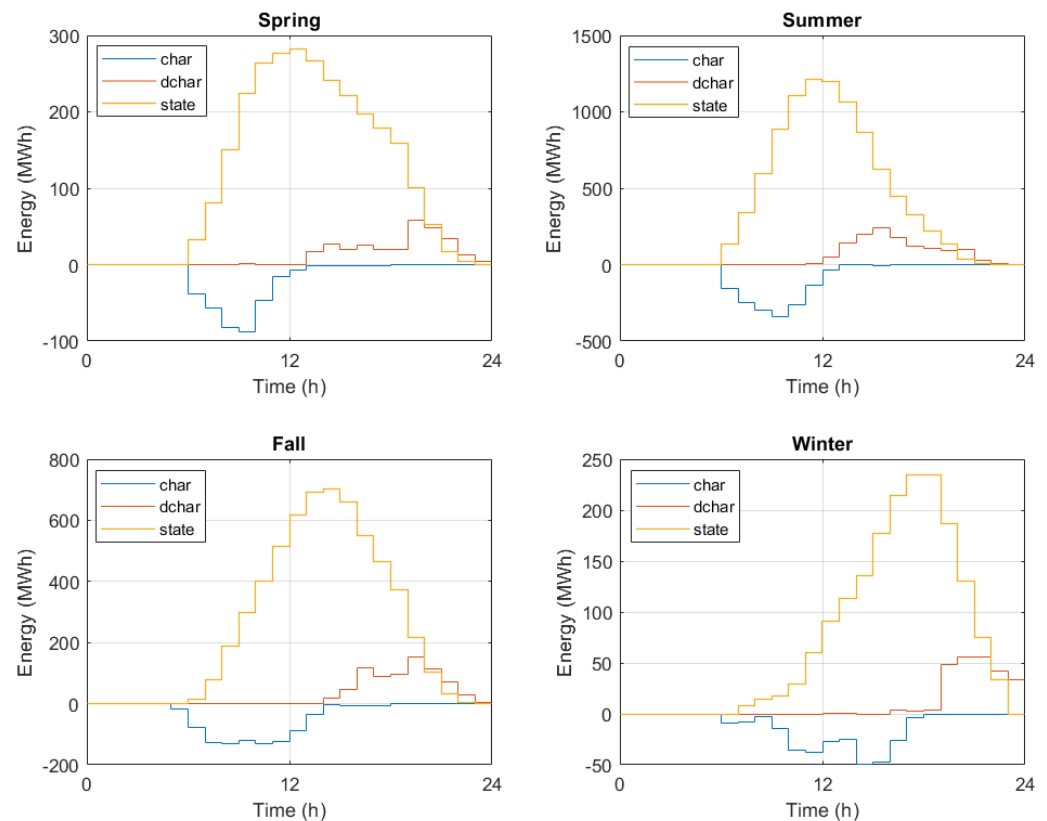


**Figure 3.** Charging/discharging operations and stored energy in the system.

#### 4.3. Load Profile

In this simulation, a net load profile with BESS installation is achieved by subtracting wind and solar PV generation from the averaged load profile plus discharging power from the BESSs. In Figure 4, the peak load is shaved. Instead, the net loads before the times 13:00, 12:00, and 15:00 are increased for spring, summer, and fall, respectively, when compared with those without the BESS installation. In winter, double load peaks are observed, and the highest peak during the evening is shaved. The net load is increased during the low load period from 11:00 to 19:00 in the situation of BESS operation, which leads to narrowing down the gap between the peak and base loads.

The power system simulated indicates a high portion of installed solar PV capacity, reaching 14.55% of the total generation capacity. One drawback associated with the high share of solar PVs in the generation mix is frequently addressed as the “duck curve”, which indicates a deep sag of the net load profile around the middle of a day due to high penetration of solar power generation and low load level. Based on Figure 4, it can be observed that the deep sag is slightly mitigated during daytime by the operations of BESSs.

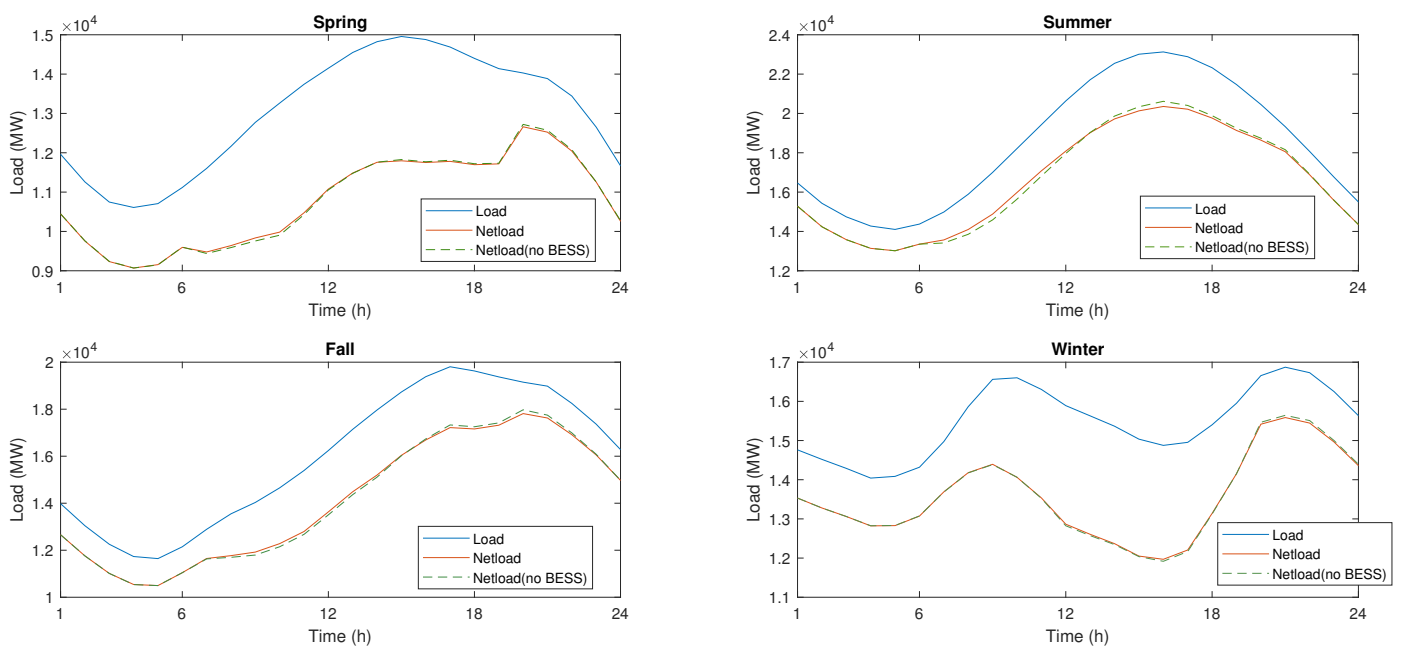


**Figure 4.** Net load curves for the seasons. The dotted lines indicate net loads without BESSs.

#### 4.4. Impacts of Stochastic Parameters

An optimal solution to the given stochastic problem is an approximated solution obtained with a finite number of sample paths, where the uncertainty realization is represented by the finite number of random sample paths. It remains unclear how the solution is affected when the uncertainty is included in the optimization problem and how we can quantify that. In this section, the idea of VSS is employed [14], which measures the impact of considering stochastic factors by evaluating the difference between objective values with and without considering stochastic parameters in the optimization model.

VSS can be calculated as  $VSS = EEV - RP$ , where  $EEV$  indicates the “expected result of using the EV solution”, and  $RP$  indicates “the solution to the recourse problem”. The EV solution indicates the optimal solution obtained using the expected value of sample paths. VSSs with 10, 20, and 30 sample paths are compared in Table 5 to verify the changes of VSSs as the number of sample paths changes. The EV solutions suggest that building BESSs is not economic. Therefore, no BESS was built for 10, 20, and 30 sample paths. Based on the VSSs, it is observed that the VSS, i.e., the gap between the optimal values obtained with considering uncertainty of renewable resources and load and without considering uncertainty, is affected by the number of samples. In the case that the number of sample paths is large, the impact of considering the uncertainty in the problem becomes large.

**Table 5.** Value of stochastic solutions (\$ million/year).

Number of Samples	EEV	RP	VSS
10	3674.294	2358.81	1315.484
20	8397.132	5701.641	2695.491
30	8071.124	5079.642	2991.482

## 5. Discussion

The results discussed in Section 3.1 show the sensitivity of the optimal solutions with respect to the number of sample paths. It is observed that the building capacity and costs increase when the number of samples increases. The number of samples affects solution quality in solving stochastic optimization problems using a sample average approximation approach [29]. The approximated solution is expected to be close to the true stochastic solution when the number of scenarios is sufficiently large. However, the problem size

with a large number of scenarios dramatically increases; the problem becomes intractable consequently. The solution time with 30 sample paths was about 315,852.84 s, and it can be improved with implementing a method to reduce the solution time in the future.

Considering the uncertainty in the model can decrease the optimal objective values because of the decreased penalty costs incurred by unserved electricity demand. VSSs indicate that the solution obtained from a recourse problem has a lower objective value than the solution from the deterministic problem. It can be noted that the optimal solution to the stochastic BESS planning model implies that the uncertainty of electric loads and renewable resources are dealt with, resulting in decreased penalty costs for unserved electric loads.

## 6. Conclusions

In this paper, optimal durations and capacity of BESSs coupled with solar PVs have been examined for a transmission-level power system when a high portion of solar PV generating units exist. The BESSs can store energy only from the solar PV generators and supply energy to the grid as needed. The mathematical model for the simulation is based on stochastic linear programming that the decision variables are represented by continuous variables to deal with a huge computational burden. The solar DNI, wind power availability, and electric load are defined as uncertain factors in the optimization model. The uncertain parameters are represented by the ARTA processes, which generate random sample paths representing time sequence as well as uncertainty. Therefore, the second stage operating problem considers chronology and hourly status of the system components.

The optimization model was applied to the high voltage 300-bus system, minimizing the total cost with satisfying all the physical constraints, such as DC power flow, capacity limits of transmission lines and generators. With the constraint to enforce at least 20% electric energy from renewable sources, the optimal solution ensures renewable generation at a target level. The key role of BESSs in bulk power systems may decrease the gap between peak load and off-peak load using electric energy from solar PV systems, with optimally arranged operating schedules of BESSs.

**Funding:** This work was supported by the National Research Foundation of Korea (NRF) grant funded by the Korea government (MSIP; Ministry of Science, ICT & Future Planning) (No. 2020R1F1A1064957).

**Institutional Review Board Statement:** Not applicable.

**Informed Consent Statement:** Not applicable.

**Data Availability Statement:** No new data were created or analyzed in this study. Data sharing is not applicable to this article.

**Conflicts of Interest:** The author declares no conflict of interest.

## References

1. Energy Storage Technology and Cost Characterization Report. Available online: [https://www.energy.gov/sites/prod/files/2019/07/f65/StorageCostandPerformanceCharacterizationReport\\_Final.pdf](https://www.energy.gov/sites/prod/files/2019/07/f65/StorageCostandPerformanceCharacterizationReport_Final.pdf) (accessed on 11 January 2021).
2. Oudalov, A.; Cherkaoui, R.; Beguin, A. Sizing and optimal operation of battery energy storage system for peak shaving application. In Proceedings of the 2007 IEEE Lausanne Power Tech, Lausanne, Switzerland, 1–5 July 2007; [CrossRef]
3. Lu, B.; Shahidehpour, M. Short-term scheduling of battery in a grid-connected PV/battery system. *IEEE Trans. Power Syst.* **2005**, *20*, 1053–1061. [CrossRef]
4. Hosseinalizadeh, R.; Shakouri, H.; Amalnick, M.S.; Taghipour, P. Economic sizing of a hybrid (PV–WT–FC) renewable energy system (HRES) for stand-alone usages by an optimization-simulation model: Case study of Iran. *Renew. Sustain. Energy Rev.* **2016**, *54*, 139–150. [CrossRef]
5. Zhang, Y.; Lundblad, A.; Campana, P.E.; Benavente, F.; Yan, J. Battery sizing and rule-based operation of grid-connected photovoltaic-battery system: A case study in Sweden. *Energy Convers. Manag.* **2017**, *133*, 249–263. [CrossRef]
6. Xia, S.; Chan, K.; Luo, X.; Bu, S.; Ding, Z.; Zhou, B. Optimal sizing of energy storage system and its cost-benefit analysis for power grid planning with intermittent wind generation. *Renew. Energy* **2018**, *122*, 472–486. [CrossRef]
7. Talent, O.; Du, H. Optimal sizing and energy scheduling of photovoltaic-battery systems under different tariff structures. *Renew. Energy* **2018**, *129*, 513–526. [CrossRef]

8. Zebarjadi, M.; Askarzadeh, A. Optimization of a reliable grid-connected PV-based power plant with/without energy storage system by a heuristic approach. *Sol. Energy* **2016**, *125*, 12–21. [[CrossRef](#)]
9. Xu, L.; Ruan, X.; Mao, C.; Zhang, B.; Luo, Y. An improved optimal sizing method for wind-solar-battery hybrid power system. *IEEE Trans. Sustain. Energy* **2013**, *4*, 774–785. [[CrossRef](#)]
10. Hemmati, R.; Saboori, H. Stochastic optimal battery storage sizing and scheduling in home energy management systems equipped with solar photovoltaic panels. *Energy Build.* **2017**, *152*, 290–300. [[CrossRef](#)]
11. Jabr, R.A.; Džafić, I.; Pal, B.C. Robust optimization of storage investment on transmission networks. *IEEE Trans. Power Syst.* **2015**, *30*, 531–539. [[CrossRef](#)]
12. Chowdhury, N.; Pilo, F.; Pisano, G. Optimal energy storage system positioning and sizing with robust optimization. *Energies* **2020**, *13*, 512. [[CrossRef](#)]
13. U.S Energy Information Administration. Short-Term Energy Outlook. Available online: [https://www.eia.gov/outlooks/steo/pdf/steo\\_full.pdf](https://www.eia.gov/outlooks/steo/pdf/steo_full.pdf) (accessed on 11 January 2021).
14. Birge, J.R.; Louveaux, F. *Introduction to Stochastic Programming*; Springer: New York, NY, USA, 1997.
15. Cario, M.C.; Nelson, B.L. Autoregressive to anything: Time-series input processes for simulation. *Oper. Res. Lett.* **1996**, *19*, 51–58. [[CrossRef](#)]
16. Cario, M.C.; Nelson, B.L. Numerical methods for fitting and simulating Autoregressive-to-Anything processes. *Inform. J. Comput.* **1998**, *10*, 72–81. [[CrossRef](#)]
17. Park, H. Generation capacity expansion planning considering hourly dynamics of renewable resources. *Energies* **2020**, *13*, 5626. [[CrossRef](#)]
18. Shapiro, A.; Dentcheva, D.; Ruszczyński, A. *Lectures on Stochastic Programming*; MPS-SIAM: Philadelphia, PA, USA, 2009.
19. Duffie, J.A.; Beckman, W.A. *Solar Engineering of Thermal Processes*; Wiley: New York, NY, USA, 2013.
20. Park, H.; Baldick, R. Optimal capacity planning of generation system integrating uncertain solar and wind energy with seasonal variability. *Electr. Power Syst. Res.* **2020**, *180*, 106072. [[CrossRef](#)]
21. North American Electric Reliability Corporation. M-1 Reserve Margin. Available online: <https://www.nerc.com/pa/RAPA/ri/Pages/PlanningReserveMargin.aspx> (accessed on 11 January 2021).
22. Ran Fu and Timothy Remo and Robert Margolis. 2018 U.S. Utility-Scale Photovoltaics-Plus-Energy Storage System Costs Benchmark. 2018. Available online: <https://www.nrel.gov/docs/fy19osti/71714.pdf> (accessed on 11 January 2021).
23. Cole, Wesley and Frazier, Allister. Cost Projections for Utility-Scale Battery Storage. 2019. Available online: <https://www.nrel.gov/docs/fy19osti/73222.pdf> (accessed on 11 January 2021).
24. U.S. Energy Information Administration. Annual Energy Outlook 2019. 2020. Available online: <https://www.eia.gov/outlooks/archive/aeo19/> (accessed on 11 January 2021).
25. Illinois Center for a Smarter Electric Grid. IEEE 300-Bus System. Available online: <http://icseg.iti.illinois.edu/ieee-300-bus-system/> (accessed on 11 January 2021).
26. University of Washington. Power Systems Test Case Archive. Available online: [https://www2.ee.washington.edu/research/pstca/pf300/pg\\_tca300bus.htm](https://www2.ee.washington.edu/research/pstca/pf300/pg_tca300bus.htm) (accessed on 11 January 2021).
27. SolarAnywhere. Available online: <https://www.solaranywhere.com/> (accessed on 11 January 2021).
28. GAMS Documentation 33. Available online: [https://www.gams.com/latest/docs/S\\_CPLEX.html](https://www.gams.com/latest/docs/S_CPLEX.html) (accessed on 11 January 2021).
29. Park, H.; Baldick, R.; Morton, D.P. A stochastic transmission planning model with dependent load and wind forecasts. *IEEE Trans. Power Syst.* **2015**, *30*, 3003–3011. [[CrossRef](#)]